Check for updates

Photocatalytic degradation of methylene blue by a cocatalytic PDA/TiO$_2$ electrode produced by photoelectric polymerization

Zehui Guo,[a] Guoqing Wang, [iD] *[a] Haiqing Fu,[a] Peiqing Wang,[b] Jianhe Liao[a] and Aimin Wang[a]

This study reports a new method for photocatalysts to degrade organic dyes on organic semiconductors. A novel strategy is reported to form TiO$_2$ nanorod (NR)/polydopamine (PDA) electrodes with a photoelectric polymerization strategy for PDA (pep-PDA) to produce cocatalytic electrodes. Amperometric *i–t* curves and UV-vis diffuse reflectance spectra were recorded and showed that compared with traditional self-polymerization (sp-PDA) and electropolymerization (ep-PDA), TiO$_2$ NR/pep-PDA exhibited an enhanced photocatalytic activity under visible light. As expected, TiO$_2$ NR/pep-PDA showed a significant improvement for the degradation of methylene blue (MB) under visible light, which can be attributed to the strong absorption of PDA in the visible light region and the more complete and uniform coverage of the TiO$_2$ NRs by the pep-PDA film. This study not only proposes a novel and highly efficient way to load PDA on TiO$_2$ NRs but also provides useful insights for the loading of other photocatalysts on organic semiconductors to degrade organic dyes.

Introduction

Currently, a shortage of global fresh water resources and a deterioration of water quality have become universal problems.[1,2] An urgent need for clean water resources has led to a continuous development of advanced water-treatment technologies. There are many advanced physical and chemical technologies for water pollution treatment, such as adsorption, filtration, reverse osmosis, electrocatalysis, and photocatalysis.[3–7] However, these methods have their own limitations, such as high energy consumption and incomplete processing.[8] Fortunately, the increase in research on conductive polymer nanomaterials has presented the possibility for catalysis and adsorption to be applied together in water treatment.[9,10]

In recent years, semiconductor photocatalytic technology has shown great potential in water treatment as an environmentally friendly, stable, and inexpensive treatment method.[11] Rutile TiO$_2$ nanorod arrays (NRs) are widely used as semiconductor catalysts with high catalytic activity and thermodynamic stability.[12–14] However, the wide band gap (3.02 eV) of rutile TiO$_2$ means it only works under high-energy (UV) light, which is not conducive to the

economic viability of the material. Polydopamine (PDA) is a highly effective sensitizer that can significantly improve the photocatalytic activity of rutile TiO$_2$ under visible light.[15,16] In addition, the PDA coating has also proven to be an excellent adsorbent for methylene blue (MB).[17] The methods for forming a PDA coating on TiO$_2$ NRs include water bath self-polymerization,[10] electrochemical polymerization,[18] and photopolymerization.[15] However, we found in experiments that self-polymerization and electrochemical polymerization produced nonuniform PDA coatings on the TiO$_2$ NR surfaces, which was not conducive to MB adsorption and degradation. Furthermore, traditional PDA photopolymerization requires at least 6 h to uniformly cover the surface of TiO$_2$ NRs, which is not useful when searching for a rapid and inexpensive synthesis of the required materials.

Based on these considerations, we report a method to induce the uniform polymerization of PDA on the surface of TiO$_2$ by constructing a photoelectrocatalytic system. By introducing UV light into the traditional electropolymerization process, the PDA could evenly cover the surface of TiO$_2$ NRs in 1 h under a bias voltage of 0.2 V, which is 6 times shorter than the traditional photopolymerization time. As expected, compared to self-polymerization (sp-PDA) and electropolymerization (ep-PDA), synergistic photoelectric co-catalysis polymerization PDA (pep-PDA) on the TiO$_2$ NR surface has a higher adsorption capacity and stronger catalytic performance for MB. This synergistic method for the photoelectric co-catalysis polymerization of PDA can not only quickly form a film on the surface of a semiconductor material but can also cover the electrode surface uniformly and completely. This provides potential for the

[a]State Key Laboratory of Marine Resource Utilization in South China Sea, School of Materials Science and Engineering, Hainan University, No. 58, Renmin Avenue, Haikou 570228, P. R. China. E-mail: 13208916675@163.com; 1359650458@qq.com; 990359@hainanu.edu.cn; aimwang@163.com; wangguoqing@hainanu.edu.cn; Tel: +86-898-31670103

[b]Sichuan Sunvea New Materials Co., Ltd., GuangAn, 638500, China. E-mail: 13817849388@163.com

industrial applications of TiO$_2$ NR/pep-PDA in the photocatalytic degradation of organic dyes.

Experiment

Preparation of rutile TiO$_2$ NRs

Before the hydrothermal reaction started, half of the area of the FTO was wrapped with green tape and then sequentially sonicated for 20 min in isopropyl alcohol, acetone, ethanol, and pure water. Next, 10 mL of pure water, 10 mL of hydrochloric acid (12 M), and 1 mL of titanium isopropoxide were placed in a beaker and stirred for 60 min to form a TiO$_2$ precursor solution. Subsequently, the stirred precursor solution and the processed FTO were transferred to a reaction kettle and hydrothermally treated at 160 °C for 200 min. After the reaction was cooled to room temperature, the FTO samples in the reaction kettle were collected and sequentially washed with acetone, ethanol, and pure water. Then, they were dried at room temperature. Finally, the dried samples were placed in a muffle furnace and annealed at 550 °C for 180 min at a temperature increasing rate of 2.5 °C min^{-1}.

Preparation of the TiO$_2$ NR/pep-PDA electrode

PDA was uniformly and completely grown on the surface of the TiO$_2$ NRs by introducing light during the electropolymerization (bias 0.2 V) process. Briefly, 400 mg of a dopamine (DA) hydrochloride solution was added to 100 mL of PBS (pH = 6.0) solution as an electrolytic solution. In a quartz glass beaker, a three-electrode system (Pt counter electrode and Ag/AgCl reference electrode; Zahner Zennium, Germany) was used to simulate the electropolymerization environment, and the working electrode was irradiated with a low-power UV light (30 W, 365 nm) source for 60 min. To facilitate comparisons,

a self-polymerized (90 °C, 240 min) TiO$_2$ NR/sp-PDA electrode and an electropolymerized (0.8 V, 60 min) TiO$_2$ NR/ep-PDA electrode were prepared with the same content of dopamine hydrochloride.

Adsorption of methylene blue

The prepared TiO$_2$ NR/pep-PDA electrode and 30 mL of an MB solution (0.1 mg mL^{-1}) were put into a beaker and stirred at a low speed for 360 min in darkness. The MB concentration in the supernatant was measured every 60 min using a UV-visible spectrophotometer. The initial absorbance was expressed as C_0, and the absorbance during the adsorption process was expressed as C, so $(C_0 - C)/C_0$ could approximate the adsorption efficiency. In addition, the TiO$_2$ NRs, TiO$_2$ NR/sp-PDA, and TiO$_2$ NR/ep-PDA electrodes were tested for absorbance by the same method. The above experiments were performed three times to evaluate the error of the experimental data.

Photocatalytic degradation of methylene blue

The prepared TiO$_2$ NR/pep-PDA electrode and 30 mL of the MB solution were placed in a round Petri dish and exposed to visible light (420–780 nm) under vertical irradiation for 180 min. The MB concentration in the supernatant was measured every 30 min using a UV-visible spectrophotometer. The initial absorbance was expressed as V_0, and the absorbance during the adsorption process was expressed as V, so $(V_0 - V)/V_0$ could approximate the degradation efficiency. In addition, the TiO$_2$ NRs, TiO$_2$ NR/sp-PDA, and TiO$_2$ NR/ep-PDA electrodes were tested for absorbance by the same method. The above experiments were performed three times to evaluate the error of the experimental data.
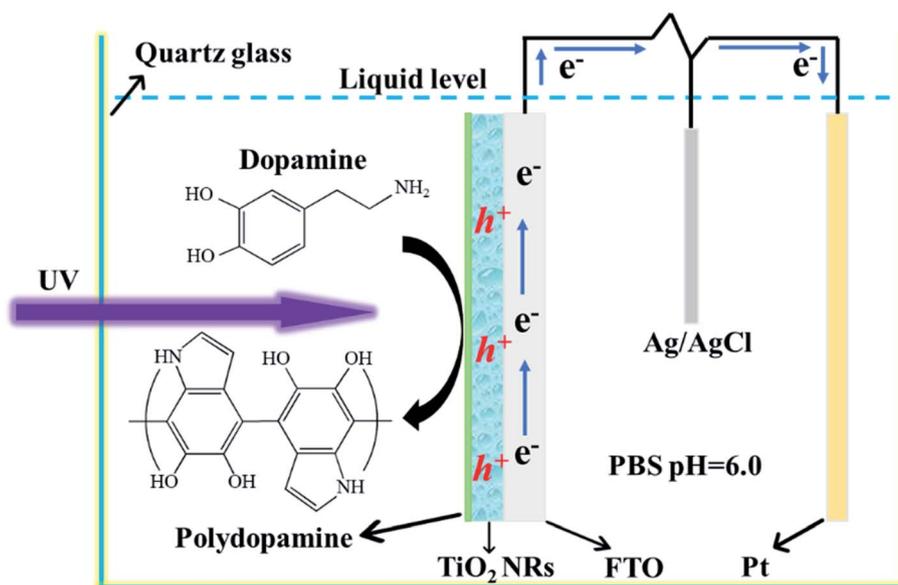

Fig. 1 Schematic of the photoelectrocatalytic polymerization of PDA on the surface of the TiO$_2$ NR electrode.

Results and discussion

Preparation and characterization

The preparation process of the TiO$_2$ NR/pep-PDA is shown in Fig. 1. According to the previously reported classical method,[19] TiO$_2$ NRs were grown on FTO by a hydrothermal reaction using titanium isopropoxide hydrochloride as a precursor. The washed and calcined TiO$_2$ NR electrodes were placed in an oven to dry. Then, the prepared TiO$_2$ NR electrode was placed in a DA solution (quartz beaker, pH = 6.0) and connected to a Pt electrode and a reference electrode through an electrochemical workstation. After the electropolymerization system was set up, the voltage was set to 0.2 V and low-power UV light was used to irradiate the conductive surface of the electrode. It is known that TiO$_2$ NR electrodes can generate a large number of holes and electrons under UV light. However, due to the high photoelectric recombination efficiency, the actual number of holes and electrons is much lower than the theoretical value, which results in a low efficiency of photopolymerized PDA. Fortunately, when an electrical circuit is introduced during photopolymerization, a large amount of holes will be left on the surface of the TiO$_2$ NR electrode because electrons are

transported to the counter electrode; thus, the above improves the polymerization efficiency of PDA.

To investigate the uniformity of the PDA films formed by different polymerization methods, all the electrodes were characterized by SEM. Fig. 2(a) shows a top-view SEM image of the TiO$_2$ NRs, Fig. 2(b) shows a side-view SEM image of the TiO$_2$ NRs. TiO$_2$ showed a regular nanorod array structure, and the membrane structure was not found on the surface. Fig. 2(c) shows the SEM image of the TiO$_2$ NR/sp-PDA. The PDA film was irregular on the surface of the TiO$_2$ NRs and was not well distributed because DA preferentially grows where the PDA aggregates during self-polymerization.[20] As shown in Fig. 2(d), the electropolymerized PDA films were stratiform and relatively more distributed on the surface of the TiO$_2$ NRs compared to those prepared with the self-polymerization method. The potentials on the surface of the TiO$_2$ NR electrode were different after being energized, which was caused by the crystallinity and size difference between each nanorod.[21] Fig. 2(e) shows an SEM image of the TiO$_2$ NR/pep-PDA electrode. Unlike sp-PDA and ep-PDA, the pep-PDA film was evenly distributed on the surfaces of the TiO$_2$ NRs. The combination of light and electricity caused a large number of holes to accumulate on the surface of each
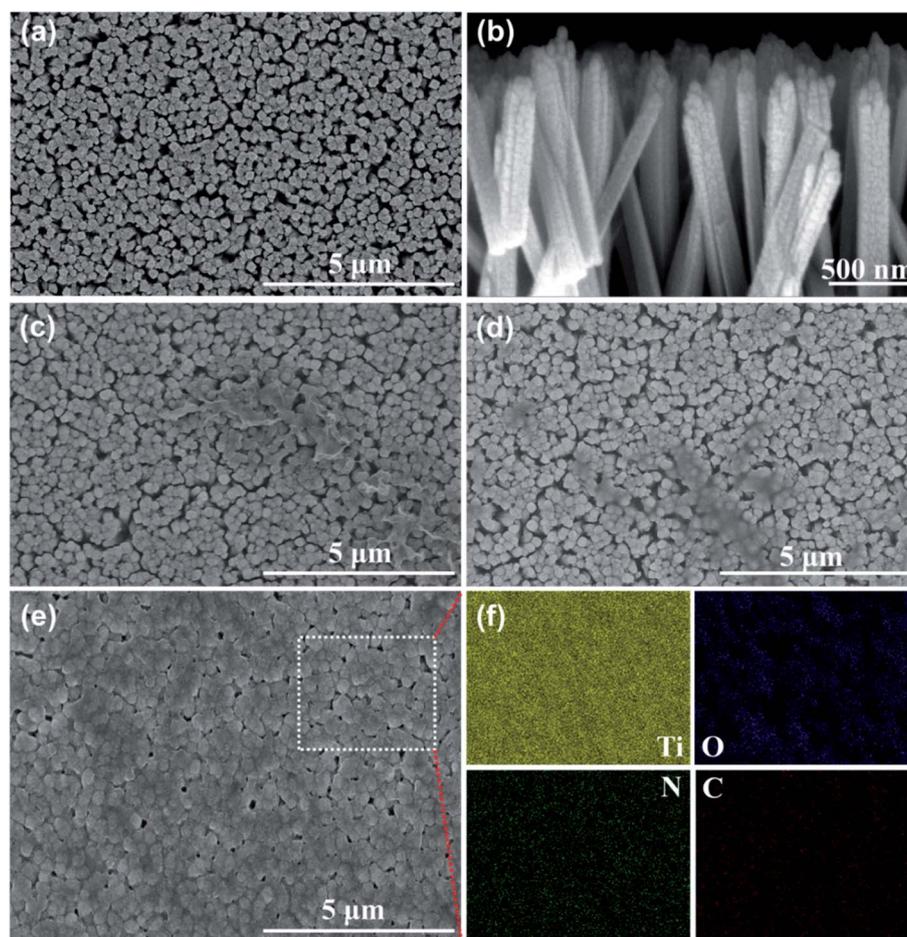

Fig. 2 Top-view SEM images of: (a) TiO$_2$ NRs, (c) TiO$_2$ NR/sp-PDA, (d) TiO$_2$ NR/ep-PDA, and (e) TiO$_2$ NR/pep-PDA. Side-view SEM images of (b) TiO$_2$ NRs. EDS mapping image of (f) TiO$_2$ NR/pep-PDA.

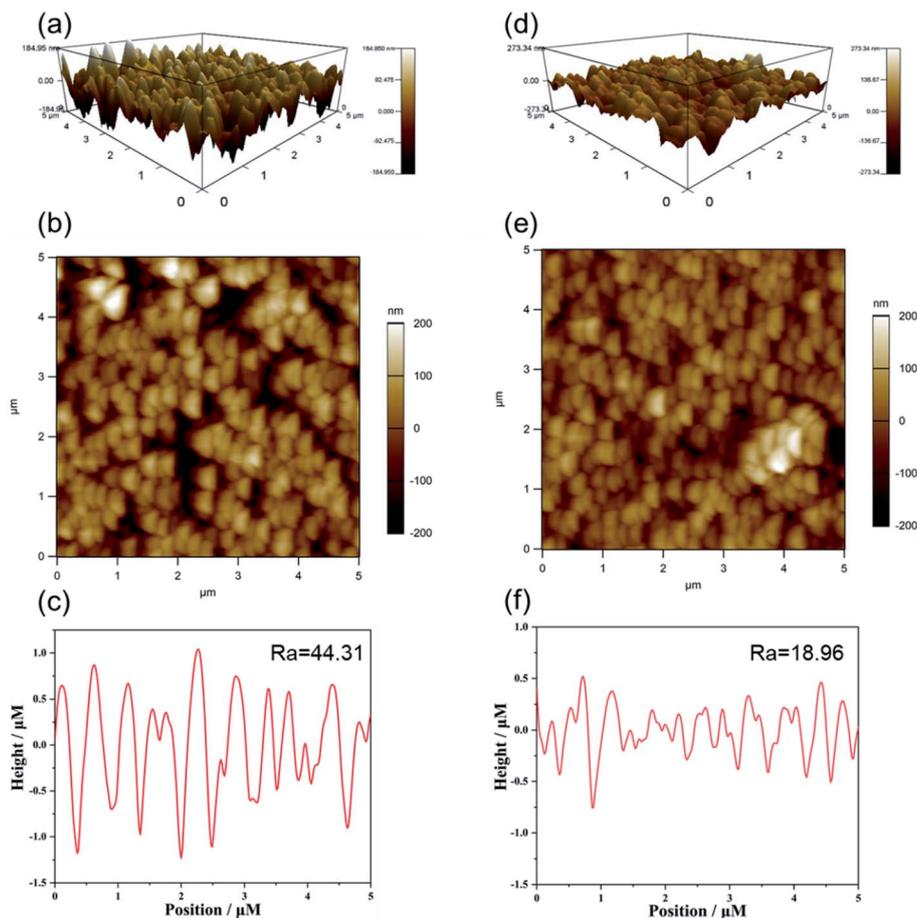**Fig. 3** 3D, 2D images and height profile of the TiO$_2$ NRs (a–c) and TiO$_2$ NR/pep-PDA (d–f) electrode generated from atomic force microscopy (AFM) analysis.

TiO$_2$ NRs. These photogenerated holes decomposed water to generate a large number of free radicals, thereby initiating the highly efficient polymerization of DA. In addition, the reason for the different thicknesses of the PDA film is that each nanorod was different from each other, so the catalytic efficiency of each place of the nanorod array was also different. To further demonstrate that the PDA film was effectively loaded on the surface of the TiO$_2$ NRs, EDS mapping characterization of the TiO$_2$ NR/pep-PDA (Fig. 2(e) white dotted area) was performed (Fig. 2(f)). Large and uniform amounts of C and N were distributed around Ti and O, which proved that the PDA film was uniformly loaded on the surface of the TiO$_2$ NRs.

Based on previous reports investigating the effect of the PDA layer on the roughness of TiO$_2$, we expected that the roughness of our synthesized TiO$_2$ NR/pep-PDA would be lower than that of TiO$_2$ NRs. The successful loading of PDA could significantly improve the roughness of materials with uneven structures. The AFM images of TiO$_2$ NRs (Fig. 3(a–c)) and TiO$_2$ NR/pep-PDA (Fig. 3(d–f)) and the roughness evaluation data are shown in Fig. 3. It can be easily seen from Fig. 3(a and d) that the electrode roughness after loading the PDA was significantly reduced. Fig. 3(c and f) show the roughness data of the electrode, where TiO$_2$ NR/pep-PDA was much smaller than TiO$_2$

NRs, which shows the uniform loading of the PDA on the electrode surface.

Comparison of the catalytic activities of the TiO$_2$ NR/PDA electrodes under different polymerization conditions

Fig. 4(a) shows the XRD patterns of the TiO$_2$ NR/PDA electrodes under different polymerization conditions. All the peaks in Fig. 4(a) are typical peaks of rutile TiO$_2$ (PDF#21-1276) and FTO (PDF#46-1088), which shows that the polymerization mode of PDA did not affect the TiO$_2$ NRs and did not introduce other impurities. The catalytic effect comes from the TiO$_2$ NRs and PDA. After 6 cycles of degradation, the crystal form and peak intensity of TiO$_2$ did not change much, indicating the stability of the TiO$_2$ NR/pep-PDA electrode.

UV-vis diffuse reflectance spectroscopy was applied to analyze the photoelectric response characteristics of the TiO$_2$ NR/PDA electrodes under different polymerization conditions. As shown in Fig. 4(b), pure TiO$_2$ had edge absorption at wavelengths lower than 420 nm. Compared with pure TiO$_2$, the spectra of TiO$_2$ NR/sp-PDA and TiO$_2$ NR/ep-PDA were enhanced in the visible region, which was attributed to the strong absorption of PDA in the visible region.[22–24] Compared with TiO$_2$ NRs/sp-PDA, the spectrum of TiO$_2$ NR/ep-PDA was significantly
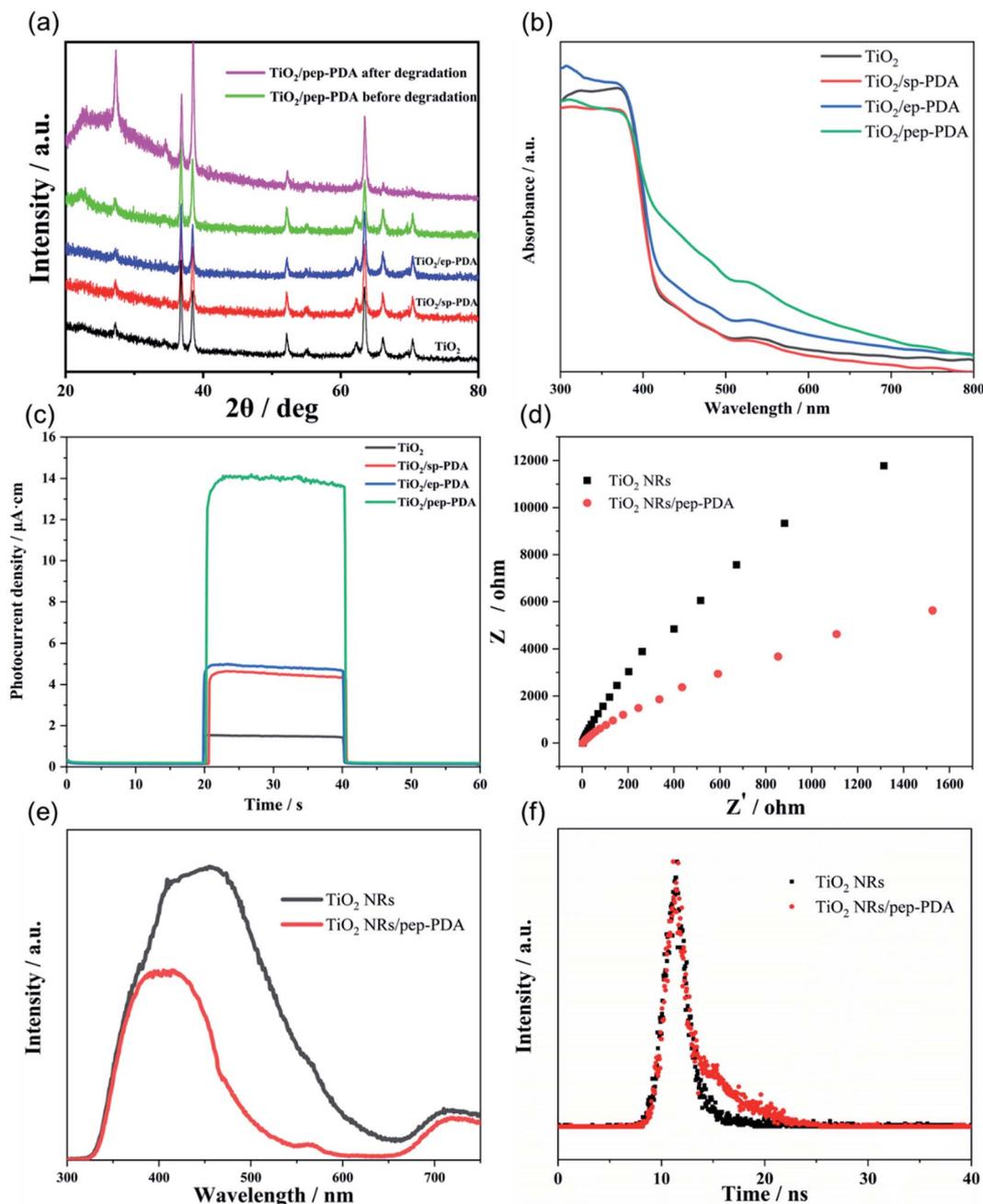
Fig. 4 (a) XRD patterns of the TiO_2 NR/PDA electrodes under different polymerization conditions and after degradation. (b) UV-vis diffuse reflection spectra and (c) amperometric $i-t$ curve responses of the TiO_2 NR/PDA electrodes under different polymerization conditions. (d) Electrochemical impedance spectroscopy (Nyquist plots) of TiO_2 NRs and TiO_2 NR/pep-PDA in the light. (e) Photoluminescence (PL) spectra under 280 nm excitation at room temperature. (f) PL decay spectra of TiO_2 NRs and TiO_2 NR/pep-PDA.

enhanced in the visible light region, which may be due to it having a more regular morphology and a more appropriate degree of PDA polymerization. It is worth noting that the spectrum of TiO_2 NR/pep-PDA had the strongest absorption in the visible light region, and the absorption band edge had a significant redshift, which indicates that pep-PDA plays a vital role in improving the visible light utilization of TiO_2 NRs.

To further understand the photocatalytic activity advantages of the TiO_2 NR/pep-PDA electrodes, instant photocurrent

measurements of the electrodes prepared with different polymerization methods were obtained by irradiation with visible light. Fig. 4(c) shows the amperometric $i-t$ curve responses of the different electrodes. The photocatalytic activity essentially corresponds to the magnitude of the photocurrent.[11,25,26] This is because the essence of photocatalysis is a redox reaction that is initiated by holes or electrons on a photoactive surface.[27,28] Therefore, to a certain extent, a high photocurrent can also represent an increase in catalytic activity. As seen from Fig. 4(c),
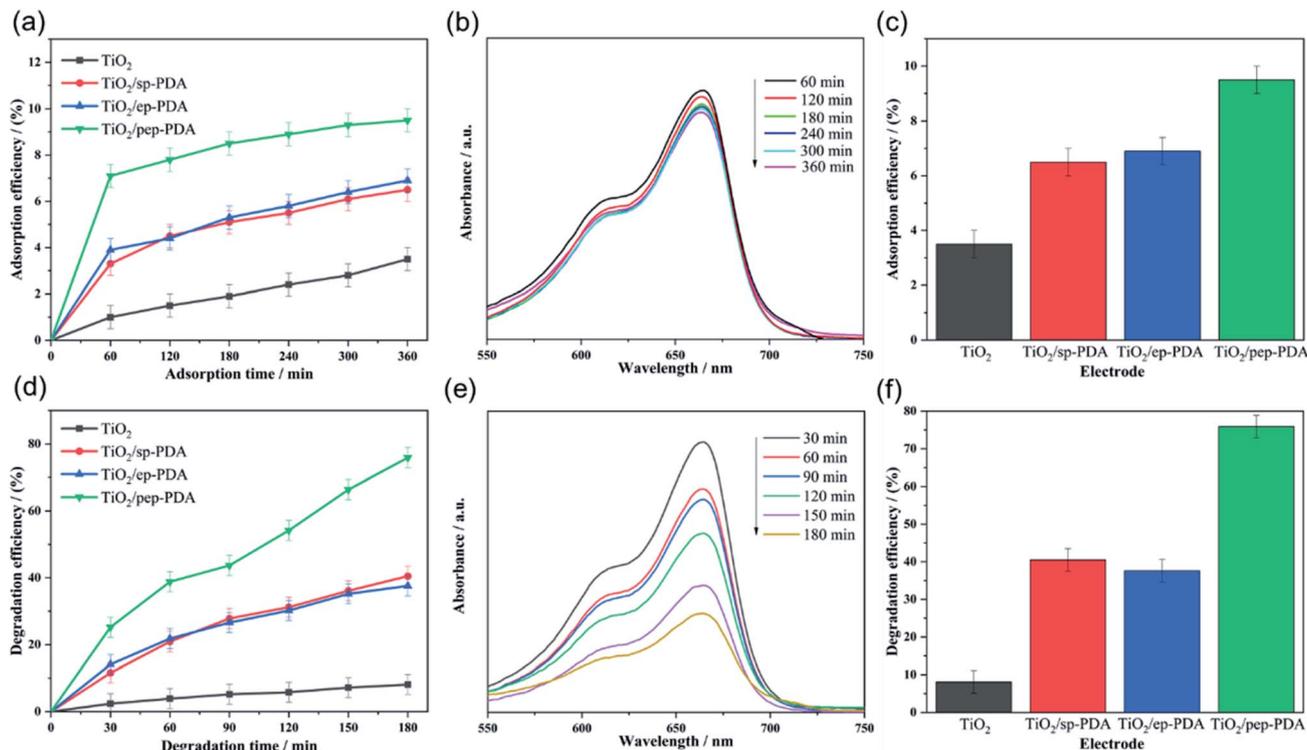
Fig. 5 (a) Adsorption efficiency of different electrodes in MB solution. (b) MB adsorption PL spectra of TiO$_2$ NRs/pep-PDA under visible light irradiation. (c) Histogram of the adsorption efficiency at 360 min. (d) Degradation efficiency of different electrodes to MB solution. (e) MB degradation PL spectra of TiO$_2$ NR/pep-PDA under visible light irradiation. (f) Histogram of the adsorption efficiency at 180 min.

the photocurrent of the TiO$_2$ NR/pep-PDA electrode was much larger than that of the other electrodes, even 10 times that of pure TiO$_2$. Therefore, pep-PDA was the most effective method for PDA loading.

As shown in Fig. 4(d), the prepared TiO$_2$ NR/pep-PDA electrodes were characterized via EIS measurement, which is a powerful strategy for detecting photoelectrons and the electron–hole separation efficiency, as well as the charge-transfer resistance of TiO$_2$ NR/pep-PDA electrodes. The radius of the semicircle in the EIS Nyquist plot was similar to the R_{ct} of the fabricated biosensor. Compared with the TiO$_2$ NRs, the TiO$_2$ NR/pep-PDA electrodes exhibited a smaller semicircle radius, higher charge-transfer efficiency, and lower R_{ct} in the same frequency range in the presence of light.[29]

Photoluminescence (PL) emission spectroscopy, which measures the irradiative recombination of electrons and holes, is a useful method to elucidate the migration and separation behavior of charge carriers in photocatalysts. We therefore measured the PL spectra for both TiO$_2$ NRs and TiO$_2$ NR/pep-PDA. The TiO$_2$ NR spectrum showed an intense and wide emission peak at about 450 nm (Fig. 4(e)). Compared to TiO$_2$ NRs, the PL emission intensity of TiO$_2$ NR/pep-PDA was much lower, indicating the increased charge separation and transfer in TiO$_2$ NR/pep-PDA.

In order to prove that the PDA introduced in TiO$_2$ could promote the separation of photogenerated electrons and holes, the photogenerated electron lifetimes of the two electrodes were

analyzed by time-resolved fluorescence spectroscopy (Fig. 4(f)). The fluorescence decay kinetics indicated that TiO$_2$ NR/pep-PDA had a longer average fluorescence lifetime, while the significantly increased average fluorescence lifetime indicated that the presence of PDA could effectively promote the separation of photogenerated electrons and holes.

MB adsorption efficiency of the TiO$_2$ NR/PDA electrodes prepared with different polymerization methods

Adsorption is also a method for treating organic pollutants. Good adsorption can assist the photoelectrode in degrading organic pollutants. Therefore, the TiO$_2$ NR/PDA electrodes produced with different polymerization methods were tested for their MB adsorption efficiency in solution. Fig. 5(a) shows the MB adsorption efficiencies of the different electrodes. It can be easily observed that the MB adsorption efficiency on the adsorbent increased rapidly in the initial stage, but then, the subsequent growth rate gradually slowed down. This result can be attributed to the fact that in the initial stage, the adsorbent has a large number of surplus adsorption sites, so it can quickly adsorb a large number of MB molecules. Then, over time, the number of adsorption sites decreases, and MB molecules on the adsorbent will also repel free MB molecules in the solution. The experimental results are thus the same as expected. The TiO$_2$ NR/pep-PDA electrode with a large area of PDA had the highest adsorption efficiency compared to that of the other two electrodes at the same time.
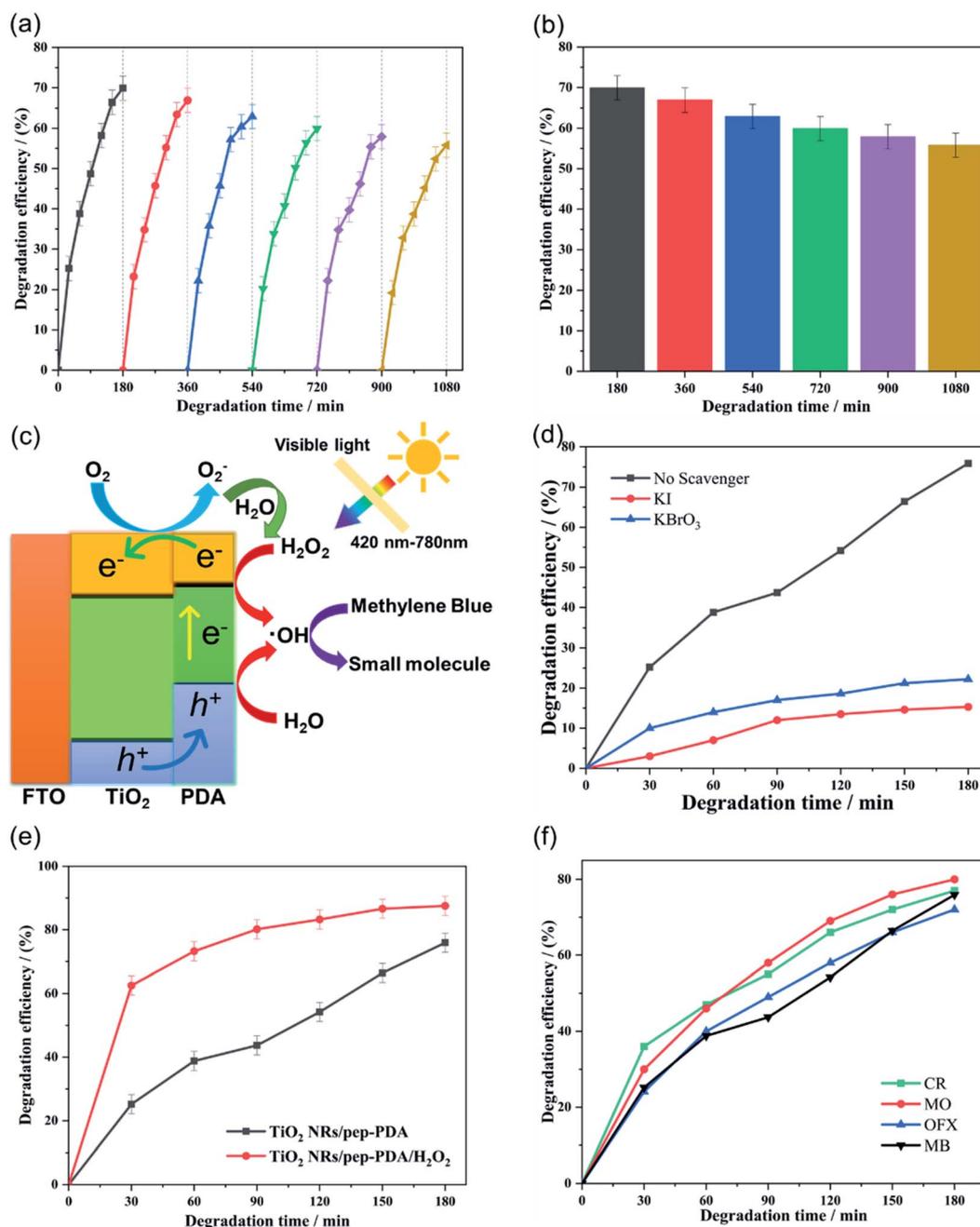
Fig. 6 (a) Measurement of the 6-cycle durability of the TiO$_2$ NR/pep-PDA electrode to MB solution. (b) Histogram of the adsorption efficiency at 180 min. (c) Photocatalytic mechanism of the TiO$_2$ NR/pep-PDA electrode to MB under visible light. (d) Effect of some scavengers on the photodegradation of MB. (e) Effect of hydroxyl radicals on the MB degradation of the TiO$_2$ NR/pep-PDA electrode. (f) Universality of the TiO$_2$ NR/pep-PDA electrode for the degradation of organic pollutants.

MB degradation efficiencies of the TiO$_2$ NR/PDA electrodes prepared with different polymerization methods

Fig. 5(d) shows the visible light catalytic performance of the four different electrode materials for MB. The TiO$_2$ NR/pep-PDA electrode, in the absence of a cocatalyst, showed enhanced visible light catalytic performance for MB, and the degradation efficiency reached 76% in 180 min. Compared with the other three electrodes, the degradation rate of TiO$_2$ NR/pep-PDA was

stable, and there was no rapid growth in the early stage or slow growth in the late stage. The reason for this may be that the degradation efficiency was limited by the electrode area.[30,31] In addition, with increasing time, the degradation efficiency of TiO$_2$ NR/ep-PDA began to decrease compared to that of TiO$_2$ NR/sp-PDA after 75 min. The reason for the above reverse trend may be that the TiO$_2$ NR/ep-PDA electrode had poor diffusibility in low-concentration MB solutions.

Considering that long-term cycle durability is one of the most important properties of photocatalysts, a stability evaluation of the TiO_2 NR/pep-PDA electrode was performed. As shown in Fig. 6(a), after 6 cycles and up to 1080 min of measurement, the TiO_2 NR/pep-PDA electrode still retained 81% of its catalytic performance when compared to the first cycle, which indicated that the prepared electrode had high stability. TiO_2 is a light and stable material, which can ensure that the catalytic ability does not significantly decrease after long-term light exposure.[32–34] Similarly, benefitting from the pep-PDA polymerization method, the uniform loading of PDA on the surface of TiO_2 is also one of the reasons for the overall performance of the stable material. Therefore, the photoelectrocatalytic polymerization of PDA is a promising method.

At present, it is generally accepted that the mechanism of degrading organic pollutants is that the free radicals generated by the photocatalytic decomposition of water react with the target molecules. Therefore, the presence of H_2O_2 is beneficial to the photocatalytic degradation process because it can be reduced by photogenerated electrons to increase the rate of free radical formation. In addition, the consumption of photogenerated electrons by H_2O_2 reduces the recombination rate of electron holes and further improves the catalytic activity of the electrode itself (Fig. 6(c)).

To understand the photocatalytic degradation mechanism and the active species involved in the degradation of MB, trapping experiments using various scavengers were investigated. The prepared TiO_2 NRs/pep-PDA catalyst was used to degrade MB after the incorporation of different scavengers. Fig. 6(d) shows that after the addition of KI and $KBrO_3$, a dramatic decrease in the photodegradation efficiency was observed, indicating that both holes and electron plays a crucial role in the degradation of MB. In addition, we further studied the effect of the addition of H_2O_2 (5 mM) on the degradation efficiency. As shown in Fig. 6(e), the final degradation efficiency of the TiO_2 NR/pep-PDA electrode under visible light was 75.6%, while the degradation efficiency reached 88.2% after adding H_2O_2. This result shows that H_2O_2 can effectively improve the degradation rate and efficiency of photocatalysts for organic pollutants.

In order to verify the universality of the prepared electrode A, catalytic degradation experiments were carried out on methylene orange (MO), Congo red dye (CR), and ofloxacin (OFX) respectively. Fig. 6(f) shows the visible light catalytic performance of the four different electrode materials for MB, MO, CR, and OFX. The TiO_2 NR/pep-PDA electrode demonstrated enhanced visible light catalytic performance for MB, MO, CR, and OFX, and the degradation efficiency reached more than 73% in 180 min. It is worth noting that the degradation efficiency of organic dyes by electrode A was greater than for antibiotics, which shows that the prepared electrode was more suitable for the treatment of water pollution.

Conclusions

In summary, we successfully developed a new photoelectric polymerization strategy for PDA (pep-PDA) to quickly construct cocatalytic TiO_2 NR/pep-PDA electrodes. Compared with the TiO_2 NR/self-polymerization (sp-PDA) and TiO_2 NR/electropolymerization (ep-PDA) electrodes, the TiO_2 NR/pep-PDA electrode had a uniform and complete PDA film, and it exhibited high efficiency in conveniently degrading MB. The enhanced photocatalytic degradation ability was attributed to the surface of the TiO_2 NRs being loaded with a more complete and uniform PDA film. In addition, the presence of H_2O_2 could effectively improve the degradation rate and efficiency of the photocatalysts to organic pollutants, which was attributed to the fact that H_2O_2 as an electron acceptor could not only improve the photocatalytic activity of the electrode but could also increase the rate of free radical generation. This study provides a new strategy for PDA loading on photocatalysts, and TiO_2 NR/pep-PDA has the potential to be applied in industrial wastewater treatments.

Conflicts of interest

The authors declare that there were no conflicts of interest.

Acknowledgements

References

1 M. Hall-Spencer, R. Rodolfo-Metalpa, S. Martin, *et al.*, *Nature*, 2008, **454**(7200), 96–99.

2 D. Jiang, Y. Zhang and X. Li, *Nanoscale*, 2017, **9**(34), 12348–12352.

3 S. Wang, Y. Boyjoo, A. Choueib and Z. H. Zhu, *Water Res.*, 2005, **39**(1), 129–138.

4 S. T. Nejad, A. A. Shahrnoy, A. R. Mahjoub, N. E. Saloumahaleh and Z. Khazaee, *Environ. Sci. Pollut. Res.*, 2018, **25**(10), 9969–9980.

5 A. H. C. Khavar, G. Moussavi, A. R. Mahjoub, M. Satari and P. Abdolmaleki, *Chem. Eng. J.*, 2018, **345**, 300–311.

6 H. Fakhri, A. R. Mahjoub and H. Aghayan, *J. Nanostruct.*, 2017, **7**, 223–235.

7 J. Cao, B. Xu, H. Lin, B. Luo and S. Chen, *Chem. Eng. J.*, 2012, **185–186**, 91–99.

8 M. S. Sajab, C. H. Chia, S. Zakaria and P. S. Khiew, *Bioresour. Technol.*, 2013, **128**, 571–577.

9 K. Ai, Y. Liu, C. Ruan, L. Lu and G. M. Lu, *Adv. Mater.*, 2013, **25**(7), 998–1003.

10 W. X. Mao, X. J. Lin, W. Zhang, *et al.*, *Chem. Commun.*, 2016, **52**(44), 7122–7125.

11 M. N. Chong, B. Jin, C. W. Chow and C. Saint, *Water Res.*, 2010, **44**(10), 2997–3027.

12 X. Wang, H. Wang, H. Zhang, *et al.*, *ACS Energy Lett.*, 2018, **3**(5), 1159–1164.

13 J. Schneider, M. Matsuoka, M. Takeuchi, *et al.*, *Chem. Rev.*, 2014, **114**(19), 9919–9986.

14 R. Li, Y. Weng, X. Zhou, *et al.*, *Energy Environ. Sci.*, 2015, **8**(8), 2377–2382.

15 Y. Liu, K. Ai and L. Lu, *Chem. Rev.*, 2014, **114**(9), 5057–5115.

16 W. Yang, W. Xu, N. Zhang, X. Lai, J. Peng, Y. Cao and J. Tu, *J. Mater. Sci.*, 2020, **55**, 6105–6117.

17 J. Fu, Z. Chen, M. Wang, *et al.*, *Chem. Eng. J.*, 2015, **259**, 53–61.

18 S. Y. Lee, S. Y. Lim, D. Seo and J.-Y. Lee, *Adv. Energy Mater.*, 2016, **6**(11), 1502207.

19 X. Li, J. Yu and M. Jaroniec, *Chem. Soc. Rev.*, 2016, **45**(9), 2603–2636.

20 F. Bernsmann, V. Ball, F. Addiego, *et al.*, *Langmuir*, 2011, **27**(6), 2819–2825.

21 J. Cai, J. Huang, M. Ge, *et al.*, *Small*, 2017, **13**(19), 1604240.

22 H. Cheng, M. Hu, Q. Zhai, S. Li and Y. Jiang, *Chem. Eng. J.*, 2018, **347**, 703–710.

23 J. Cai, J. Huang and Y. Lai, *J. Mater. Chem. A*, 2017, **5**(31), 16412–16421.

24 Y. Wei, J. Kong, L. Yang, *et al.*, *J. Mater. Chem. A*, 2013, **1**(16), 5045–5052.

25 X. Chen, S. Shen and L. Guo, *Chem. Rev.*, 2010, **110**(11), 6503–6570.

26 H. Tong, S. Ouyang, Y. Bi, N. Umezawa, M. Oshikiri and J. Ye, *Adv. Mater.*, 2012, **24**(2), 229–251.

27 G. Williams, B. Seger and P. V. Kamat, *ACS Nano*, 2008, **2**(7), 1487–1491.

28 T. Hisatomi, J. Kubota and K. Domen, *Chem. Soc. Rev.*, 2014, **43**(22), 7520–7535.

29 W. Yang, X. Wang, W. Hao, Q. Wu, J. Peng, J. Tu and Y. Cao, *J. Mater. Chem. B*, 2020, **8**, 2363–2370.

30 R. Asahi, T. Morikawa, T. Ohwaki, K. Aoki and Y. Taga, *Science*, 2001, **293**(5528), 269–271.

31 S. Liu, J. Yu and M. J. Fu, *J. Am. Chem. Soc.*, 2010, **132**(34), 11914–11916.

32 M. Pelaez, N. T. Nolan, S. C. Pillai, *et al.*, *Appl. Catal., B*, 2012, **125**, 331–349.

33 X. Chen and S. S. Mao, *ChemInform*, 2007, **38**(41), 9.

34 X. Chen, L. Liu, P. Y. Yu and S. S. Mao, *Science*, 2011, **331**(6018), 746–750.